International Journal on
"Technical and Physical Problems of Engineering"
(IJTPE)
Published by International Organization of IOTPE

ISSN 2077-3528
IJTPE Journal
www.iotpe.com
ijtpe@iotpe.com

December 2022 | Issue 53 | Volume 14 | Number 4 | Pages 303-311

A DISCRETE MECHANICAL MODEL FOR FREE TRANSVERS VIBRATIONS IN LARGE DISPLACEMENT OF A SIMPLY SUPPORTED TAPERED AFG BEAMS CARRYING POINT MASSES

A. Moukhliss [1, 2] A. Rahmouni [2] O. Bouksour [2] R. Benamar [3]

1. National Higher School of Electricity and Mechanics, ENSEM, Hassan II University, Oasis, Casablanca, Morocco
anass.moukhliss@ensem.ac.ma
2. Laboratory of Mechanics, Production and Industrial Engineering, LMPGI, Higher School of Technology of Casablanca, ESTC, Hassan II University, Oasis, Casablanca, Morocco, abd.rahmouni@gmail.com, bouksour2@gmail.com
3. Simulation Studies and Research Laboratory, Instrumentation and Measurements LERSIM, Mohammadia School of Engineers, Mohammed V University, Rabat, Morocco, rhali.benamar@gmail.com

Abstract- A discrete mechanical model is used to handle the non-linear free transverse vibrations of a Conical Beam manufactured from axial functional gradient material (TAFGB) supporting spot masses at several locations. The beam is modelled as a system with N degrees of freedom (N-Dof), including *N* masses, *N*+1 bars and *N*+2 spiral spring. The details of the current model are shown in the following. After the calculation of the new mass tensor (including the effect of added masses) m_{ij} , the linear stiffness tensor k_{ij} and the nonlinear stiffness tensor b_{ijkl} according to (TAFGB), Hamilton's principle is applied and results in a nonlinear algebraic system. The impact of geometric nonlinearity is then studied using a single-mode approach to obtain the associated backbone curves giving the amplitude-dependent nonlinear frequencies. The resulting ratio of dimensionless nonlinear to linear frequency, for a wide range of maximal amplitude of the considered beam is in good agreement with previously published results, which shows that validity of the present discrete model and its availability for other applications to nonuniform materials. The great adaptability of this model makes the study of the parameters very simple by easily controlling the laws of change of the geometric and physical properties of the (TAFB) as well as the location and magnitude of the point masses on the nonlinear backbone curves.

Keywords: Discrete Model, Free Vibration, Geometrically Non-Linear, AFG Beam, Point Masses, Single-Mode Approach.

1. INTRODUCTION

Due to the widespread use of mechanical systems in various sectors, such as aerospace and civil engineering, etc. Many publications deal with free and forced vibrations tensors m_{ij} , k_{ij} and b_{ijkl} are derived for the typical case which is considered a general case. The discrete nature of of known structures, beam, plate and shell… etc. See for example [1-9]. However, the study of large vibrations of conical AFG beams is not very frequent in the literature and become a major problem for researchers. A few papers [10-12] deal the vibration response of the (TAFGB) beam in large displacement.

The goal of this study is to develop a discrete model presented by Rahmouni, Khnaijar, Moukhliss and Benamar [9], [13-16] to handle the geometrically nonlinear transvers free vibrations of Conical Beam made of axial functional gradient material carrying point masses in various location, and that considers the effect of various factors on the dynamic responses of the (TAFGB), in particular the taper ratio, the laws describing the geometrical and physical properties along the length, the magnitude and the location of point masses.

The beam is modeled as an N-Dof system including *N* masses of magnitude m_r modeling the inertia of the beam and connected by means of *N*+1 bars of an infinite stiffness. The discrete system includes *N*+2 spiral springs of rigidity C_r^l simulating the flexural stiffness of the beam. The geometrical nonlinearity due to the large displacements caused by the normal forces is modeled by *N*+1 linear springs of stiffness k_r . Note that the elements m_r , C_r^l and k_r vary in the length direction because of the inhomogeneity of the beam under study, this variation is governed by the laws presenting the distribution along the length of the (TAFGB) of the geometric and physical properties. Note that the total mass of the (TAFGB) is non-uniformly distributed among the *N* masses, this is guided by the laws of density and cross-sectional change along the *x*-axis of the beam.

The nature of the typical tapered beams used in this work is a symmetrical two-step bilinear tapered beam, the this model makes it easier to study of the other types of beams in particular linearly tapered, parabolically conical and exponentially conical, etc. Different material and

property laws are examined as well as the effect of adding and magnitude point masses on the vibratory behavior in large amplitude of the considered beam.

The new tensors, m_{ij} , k_{ij} and b_{ijkl} are calculated using the same steps presented in [14, 15]. A transition is made from (D-B) displacement basis, to (M-B) modal basis. We apply Hamilton's principle we find a nonlinear algebraic system. The single-mode approach allows to predict rather precisely the nonlinear frequency response curve in the proximity of the first resonance [17]. In the following paragraphs we present details on the discrete model, and the expressions of the new tensors m_{ij} , k_{ij} and b_{ijkl} a function of the geometric and physical characteristics of the (TAFGB).

2. GENERALE FORMULATION AND NOMENCLATURE

The model we used is the one elaborated by Rahmouni [14]. We present in this work our contribution by adapting this model to handle the geometrically nonlinear free vibrations of non-uniform and non-homogeneous beams.

2.1. Description of the Discrete Model

In this work, the discrete mechanical model is applied to address the nonlinear free vibrations of a beam with variable geometrical parameters made of a material of axial functional gradient. Only one nonlinearity is considered, the geometric nonlinearity resulting from the induced axial force due to the large deformations. The geometrical and physical parameters namely length, density, squared moment, cross-sectional area, and Young's modulus are denoted respectively by $L, \rho(x), I(x), A(x)$ and $E(x)$. The widths and heights of the sections located at $x=-\frac{L}{2},0$ and $\frac{L}{2}$ are noted respectively by $\left(h_{left};b_{left}\right)$, $\left(h_0;b_0\right)$, $\left(h_{right};b_{right}\right)$. The typical tapered beam is composed of two steps assumed geometrically symmetrical with respect to the middle of the beam such that $h_{left}=h_{right}$, $b_{left}=b_{right}$ and the same length $L_1=L_2=\frac{L}{2}$ as shown in Figure 1.

The considered beam is modeled by a discrete mechanical system composed of N masses $m_1,...,m_r,...,m_N$ for $r=1,...,N$ whose values depend on the position of each mass because of the non-uniform nature of the beam, these last ones are linked between them through $N+1$ bars of infinite rigidities, of negligible masses and inertias. We place $N+1$ longitudinal linear springs of stiffness $k_1,...,k_r,...,k_{N+1}$ for $r=1,...,N+1$ whose value depends on the location of each bar; these last ones modeled the geometrical non-linearity due to the big amplitudes caused by the normal forces induced in the beam. The flexural rigidity is modelled is modeled by N+2 spiral Springs of moment $M_f=C_r^l\Delta\theta$ and stiffness $C_1^l,...,C_r^l,...,C_{N+2}^l$ for $r=1,...,N+2$. The values of C_1^l and C_{N+2}^l are assumed to be zero for simply supported extremities [18]. We note by n_M the number of concentric masses in the beam and x_n the x-coordinate of the mass n. We present in Figure 2, the projection of the beam in the (x, y) plane and the corresponding discrete model.

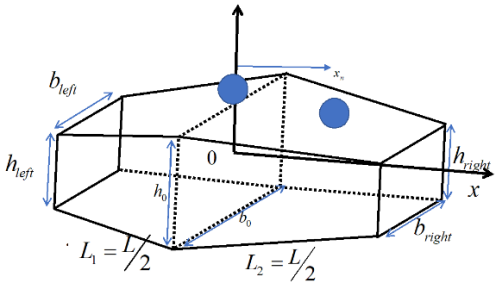

Figure 1. The typical (TAFGB) containing two masses

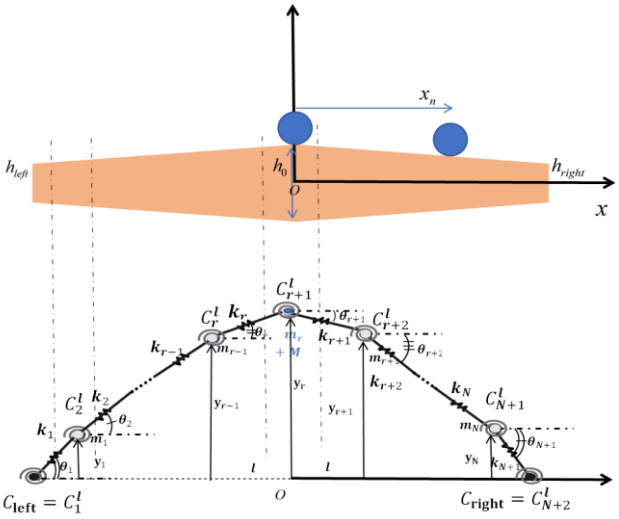

Figure 2. Bi-linear tapered AFG beam and the corresponding discrete multi-degree of freedom system

The beam shown in Figure 1 is similar to the one presented in [19] the thickness and width of the (TAFGB) are given by the following Equations:

$$h(x)=\begin{cases} h_1(x)=h_0\left(1+\alpha\frac{2x}{L}\right)^e & -\frac{L}{2}\le x\le 0 \\ h_2(x)=h_0\left(1-\alpha\frac{2x}{L}\right)^e & 0\le x\le\frac{L}{2}\end{cases} \quad (1)$$

$$b(x)=\begin{cases} b_1(x)=b_0\left(1+\alpha\frac{2x}{L}\right)^p & -\frac{L}{2}\le x\le 0 \\ b_2(x)=b_0\left(1-\alpha\frac{2x}{L}\right)^p & 0\le x\le\frac{L}{2}\end{cases} \quad (2)$$

The expression of the cross section of each portion and the square moment are given by the following expressions:

$$A_{1,2}(x_r)=A_0\left(1\pm\alpha\frac{2x_r}{L}\right)^{p+e} \quad (3)$$

$$I_{1,2}(x_r)=I_0\left(1\pm\alpha\frac{2x_r}{L}\right)^{p+3e} \quad (4)$$

The location of the mass m_r on the x-axis is illustrated by $x_r=-L/2+(r-1)\times l$ as shown in Figure 2. With $r=1,\ldots,(N+1)/2+1$ for the left part of the beam i.e. for $-L/2<x<0$ (index 1). For the other part, $r=(N+1)/2+1,\ldots,N+2$ related to $0<x<L/2$ (index 2), where $l=L/(N+1)$ is the space used to separate two successive masses. We choose an odd number of N-Dof to take into account the mechanical behavior of the section located in the middle in the calculation, it amounts to inject the compatibility conditions automatically in the study.

We can find the useful expressions of the geometrical parameters $h(x), b(x), A(x), I(x)$ and $E(x)$ of the beam for 3 particular cases.

- Beam 1: Corresponds to the general case of a bilinear tapered beam such that (e=p=1).
- Beam 2: Corresponds to a tapered beam with a rectangular section of constant width and linearly varying depth, $b_1(x)=b_2(x)$, which leads to (e=1 and p=0).
- Beam 3: Corresponds to a beam of linearly varying width and constant depth, $h_1(x)=h_2(x)$ (e=0 and p=1).

2.2. Expression of T, V_l and V_{nl} of the N-Dof System

The expressions for the linear potential energy, the kinetic energy, and nonlinear potential energy (translating the geometric nonlinearity) of system at N-Dof are denoted respectively by V_l , T and V_{nl} are defined by the following relations [14]:

$$V_l = \frac{1}{2} y_i y_j k_{ij}(x) \tag{5}$$

$$V_{nl} = \frac{1}{2} y_i y_j y_k y_l b_{ijkl} \tag{6}$$

$$T = \frac{1}{2} \dot{y}_i \dot{y}_j m_{ij}(x) \tag{7}$$

where, i, j, k, l are indices varying from 1 to N.

The expression for the amplitude of the mass i in (D-B) is given by [14].

$$y_i(t) = A_i \cos\left(\omega_{Ndof}^{nl} t\right) \quad i, j = 1,\ldots,N \tag{8}$$

$$y_i(t) = \varphi_{ij} a_j \cos\left(\omega_{Ndof}^{nl} t\right) \quad i, j = 1,\ldots,N \tag{9}$$

where, $[\varphi] = \left[\{\varphi_{1i}\}\{\varphi_{2i}\},\ldots,\{\varphi_{Ni}\}\right]$ is the passage matrix of the (D-B) to (M-B) also represents the linear modes of system at N-Dof. Where A_i represents the modulus of displacement y_i in the (D-B) and a_i the modulus of displacement in the (M-B). The ω_{Ndof}^{nl} is the nonlinear frequency of the discrete system associate with the amplitude A_i .

We can rewrite the expressions of energies by replacing Equation (9), respectively in (5)-(7) we find as in [14].

$$V_l = \frac{1}{2} a_i a_j \bar{k}_{ij}(x_i) \cos^2\left(\omega_{Ndof}^{nl} t\right) \tag{10}$$

$$V_{nl} = \frac{1}{2} a_i a_j a_k a_l \bar{b}_{ijkl}(x_i) \cos^4\left(\omega_{Ndof}^{nl} t\right) \tag{11}$$

$$T = \frac{1}{2} a_i a_j \left(\omega_{Ndof}^{nl}\right)^2 \bar{m}_{ij}(x_i) \sin^2\left(\omega_{Ndof}^{nl} t\right) \tag{12}$$

where, i, j, k, l are indices varying from 1 to N, and $\bar{m}_{ij}$, $\bar{k}_{ij}$ and $\bar{b}_{ijkl}$, are written in the (M-B).

These tensors depend on the laws of variations of the geometrical and physical parameters of the considered beam. The relations among the tensor terms in (D-B) and (M-B) are given by the following [14]:

$$\bar{k}_{ij} = \Phi_{si}\Phi_{tj}k_{st} \tag{13}$$

$$\bar{b}_{ijkl} = \Phi_{si}\Phi_{tj}\Phi_{pk}\Phi_{ql}b_{stpq} \tag{14}$$

$$\bar{m}_{ij} = \Phi_{si}\Phi_{tj}m_{st} \ , \ i, j = 1,\ldots,N \tag{15}$$

where, i, j, k, l are indices varying from 1 to N.

Using Hamilton's principle and spectral analysis [14], we can write:

$$\delta \int_0^{2\pi/\omega} (V_l + V_{nl} - T)dt = 0 \tag{16}$$

We substitute the expressions of T , V_l and V_{nl} in this Equation by their expressions presented in Equations (5)-(7), like in [14], we obtain:

$$3a_i a_j a_k \bar{b}_{ijkr} + 2a_i \bar{k}_{ir} - 2a_i \omega^2 \bar{m}_{ir} = 0 \quad , \quad i, j, k, r = 1,\ldots,N \tag{17}$$

can be expressed as a matrix as:

$$\left[\bar{K}\right]\{a\} + \frac{3}{2}\left[\bar{B}(a)\right]\{a\} - \left(\omega_{Ndof}^{nl}\right)^2\left[\bar{M}\right]\{a\} = \{0\} \tag{18}$$

where, $\left[\bar{M}\right], \left[\bar{K}\right]$, and $\left[\bar{B}(a)\right]$ showing respectively the mass matrix, the linear and non-linear elasticity matrix expressed in (M-B) and $\{a\}$ is the displacement vector in (M-B) [14]. Equation (17) is a formula describe the non-linear dynamic response of the (TAFGB). To solve it we must first establish the tensors m_{ij} , k_{ij} and b_{ijkl} . The details of the calculations are shown in next, indicating the helpful expressions of these tensors correspond to (TAFGB).

2.3. Expression of the Tensors m_{ij}, k_{ij} and b_{ijkl}

The general expression of the mass tensor is given by the formula [9], [14]:

$$m_{ii}(x) = \frac{L\rho(x_i)A(x_i)}{N+1} \quad , \quad 1 \le i \le N \tag{19}$$

$$m_{ij}(x) = 0 \quad \text{for} \quad i \ne j \quad , \quad i, j = 1,\ldots,N \tag{20}$$

where, i and j are indices varying from 1 to N.

For the portion defined in the region $-L/2 \le x \le 0$, The area of the cross-section along this portion is described by the function $A_1(x_r)$ so:

$$\begin{aligned} m_{ij}(x) &= \frac{L\rho_0 A_0}{(N+1)} \rho^*(x_i)\left(1+\alpha\frac{2x}{L}\right)^{e+p} \\ \delta_{ij} &= \frac{L\rho_0 A_0}{(N+1)} m^*(x_i)\delta_{ij} \quad \text{for} \ i, j = 1,\ldots,\frac{(N+1)}{2}+1 \end{aligned} \tag{21}$$

For the portion defined in the interval $L/2 \le x \le L$, the area of the cross section is given by the law $A_2(x_r)$.

The mass tensor components for this portion are presented as follows:

$$m_{ij}(x)=\frac{L\rho_0 A_0}{(N+1)}\rho^*(x_i)\left(1-\alpha\frac{2x}{L}\right)^{e+p}$$
$$\delta_{ij}=\frac{L\rho_0 A_0}{(N+1)}m^*(x_i)\delta_{ij} \quad \text{for } i,j=\frac{(N+1)}{2}+1...,N \tag{22}$$

If we account for the point masses. We apply a parameter η, that is defined as the ratio of the magnitude of the point mass on the abscissa x_r of a homogeneous and unvarying beam of section S_0 and of density ρ_0.

$$\eta_n=\frac{M_n}{L\rho_0 A_0} \tag{23}$$

For an added mass located at position x_r, the mass matrix can be written as follows:

$$[M(x)]=\frac{L\rho_0 A_c}{(N+1)}\begin{bmatrix} m^*(x_1) & 0 & 0 & \cdots & 0 & 0 \\ 0 & m^*(x_2) & 0 & 0 & 0 & 0 \\ 0 & 0 & \ddots & \ddots & \vdots & \vdots \\ \vdots & \vdots & \ddots & m^*(x_r)+\eta(N+1) & 0 & 0 \\ 0 & 0 & 0 & 0 & \ddots & 0 \\ 0 & 0 & 0 & \cdots & 0 & m^*(x_N) \end{bmatrix} \tag{24}$$

The expression of the k_{ij} tensor components of the system is given by [14]:

$$k_{ii}=\frac{1}{l^2}\left(C_i^l+4C_{i+1}^l+C_{i+2}^l\right),\ 1\le i\le N \tag{25}$$

$$k_{(i-1)i}=k_{i(i-1)}=-\frac{2}{l^2}\left(C_i^l+C_{i+1}^l\right),\ 2\le i\le N \tag{26}$$

$$k_{(i-2)i}=k_{i(i-2)}=\frac{1}{l^2}C_i^l,\ 3\le i\le N \tag{27}$$

The expression of coefficient C_i^l at the abscise x_i is given by:

$$C_i^l=\frac{E(x_i)I(x_i)}{l},\quad 1\le i\le N+2 \tag{28}$$

To present the nonlinear stiffness tensor corresponding to (TAFGB) we use the expression of the energy stored in the N+1 axial spring of stiffness k_i (Figure 2) modelling the geometrical nonlinearity due to the large displacement of the beam [14]:

$$V_{nl}=\sum_{i=1}^{N+1}k_i\frac{(y_i-y_{i-1})^4}{8{l_i}^2} \tag{29}$$

The expression for the stiffness k_i of the longitudinal spiral spring located at abscissa x_i is defined as follows [14]:

$$k_i=\frac{E(x_i)A(x_i)}{l_r} \quad \text{for} \quad i=1,...,N+1 \tag{30}$$

where, $l_1=l_2=l_i=...=l_{N+1}$.

As mentioned in [14], Equation (7) gives the following expressions for the terms of the nonlinear stiffness tensor (as a function of k_r) translating the geometric nonlinearity due to the deformation of longitudinal springs:

$$b_{iiii}=\frac{1}{8l^2}(k_i+k_{i+1}) \quad ,\quad 1\le i\le N \tag{31}$$

$$b_{ii-1i-1i-1}=b_{i-1ii-1i-1}=b_{i-1i-1ii-1}=$$
$$=b_{i-1i-1i-1i}=-\frac{1}{8l^2}k_i \quad ,\quad 2\le i\le N \tag{32}$$

$$b_{iiii-1}=b_{iii-1i}=b_{ii-1ii}=b_{i-1iii}=$$
$$=-\frac{1}{8l^2}k_i \quad ,\quad 2\le i\le N \tag{33}$$

$$b_{(ii-1i-1i)}=b_{(i-1ii-1i)}=b_{(i-1i-1ii)}=$$
$$=b_{(ii-1ii-1)}=b_{(i-1iii-1)}=b_{(iii-1i-1)}=\frac{1}{8l^2}k_i \tag{34}$$

where, i is varying from 2 to N. The rest of the parameters b_{ijkl} are zero.

2.4. Solution of the Nonlinear Algebraic System

The general presentation of the method of solving the algebraic system of Equation (9) is presented in [20]. The single mode approach gives the formula of the first nonlinear frequency from Equations (21), (25) and (31), the backbone curve is given by:

$$\omega_{Ndof}^{nl}=\sqrt{\frac{\bar{k}_{11}}{\bar{m}_{11}}\left(1+\frac{3}{2}a_1^2\frac{\bar{b}_{1111}}{\bar{k}_{11}}\right)} \tag{35}$$

where, a_1 is the contribution of the basic non-linear mode, written in (M-B) and used as a vibration factor.

3. RESULTS AND DISCUSSION

We present two numerical examples. The first one is for homogeneous tapered beams and the second one is for AFG tapered beams. For the two applications, we study the effect of the addition of point masses on the vibratory behavior of (TAFGB). The non-linear frequency calculations were performed using a MATLAB software.

3.1. Numerical Result 1

The beam illustrated in this example and the one presented in [21]. Three different geometries can be examined, the first one corresponds to bilinear tapered beam (Beam 1) the second one corresponds to depth tapered beam (Beam 2) and the last one match to Breth beam (Beam 3).

To justify the results of the present study, a comparison of the ratios of the non-linear and linear frequencies $\frac{\omega_{Ndof}^{*nl}}{\omega_{Ndof}^{*l}}$ is presented in Table 2 estimated for N=29 and for a large range of maximum dimensionless amplitude $A_{\max}^*=\frac{A_{\max}}{R}$, with $R=\sqrt{I_0/S_0}$ the gyration radius at x=0. The conicity parameter of the beam is noted α and is taken α =0.4. A test of the convergence of the present study is examined by presenting the fluctuation of the relative error $E_r=\left|RP_r-R[21]\right|\times 100/R[21]$ as a function of N-Dof.

Figure 3 presents the fluctuation of the relative error E_r corresponds to the (beam 2) for different values of N-

Dof and for $A^*_{\max} = 3$, we can notice that the error remains practically unchanged by increasing the N-Dof. We see that the optimal number of N-Dof is N=29.

It can be seen that the choice of N=29 allows fast execution of MATLAB program and good convergence of the results. This choice is preserved for all the applications presented in this article. As soon as the error is approximately 2%, we can assume that the results are acceptable and very reliable. Figure 4 shows the backbone curve of beam 2 for different values of α. Figure 5 shows the comparison of the backbone curve related of beam 1 and for different values of alpha α.

Table 1. Dimensionless nonlinear and linear frequency ratios for α = 0.4

$A^*_{\max}$	$\omega^{*nl}_{Ndof} / \omega^{*l}_{Ndof}$			
	Beam 2		Beam 3	
	Present Study	[21]	Present Study	[21]
0.1	1.0010	1.0010	1.0008	1.0008
0.2	1.0040	1.0042	1.0030	1.0033
0.3	1.0087	-----	1.0069	-----
0.4	1.0156	1.0166	1.0121	1.0132
0.5	1.0240	-----	1.0190	-----
0.6	1.0346	1.0370	1.0271	1.0296
0.8	1.0605	1.0649	1.0477	1.0520
0.9	1.0755	-----	1.0603	-----
1	1.0929	1.0997	1.0736	1.0801
1.2	1.1318	-----	1.1045	-----
1.5	1.1989	-----	1.1596	-----
2	1.3319	1.3354	1.2703	1.2910
2.5	1.5432	-----	1.3974	-----
3	1.6583	1.6981	1.5424	1.5811

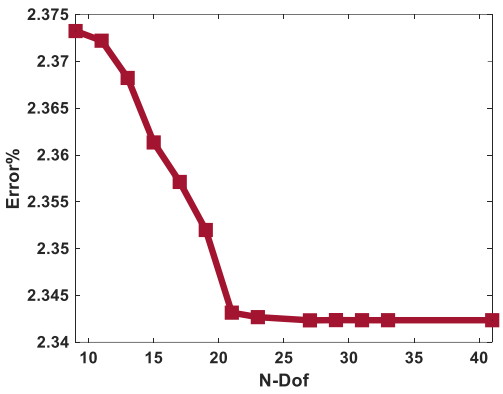

Figure 3. Relative error between the result of the present study and publish in [21]

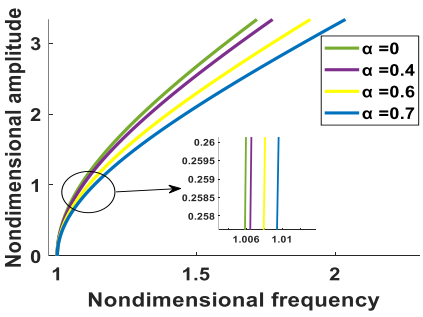

Figure 4. Comparison of the backbone curves corresponding to beam 2 for different values of α

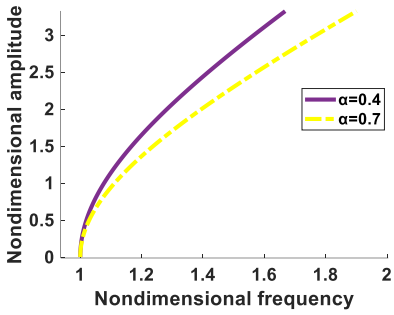

Figure 5. Comparison of the backbone curves corresponding to beam 1 for different values of α

For all examples related to the Tapered beam, it can be seen that the effect of the non-linearity increases with the increase of the coefficient describing the conicity ratios of the beam 1, 2 and 3. The nonlinearity is more significant for depth tapered than for breadth taper. In order to validate the results of the present study for the tapered beams containing point masses.

A comparison was performed with the results published in [22] for a uniform beam carrying 3-point masses i.e. $n_M = 3$, respectively in $x_n = (0.2L; 0.5L; 0.7L)$ and $\eta_n = (10;10;10)$ The results are presented as backbones curves chowing in Figure 6 whose abscissa axis match to the normalized nonlinear frequency $\omega^{nl}_{Ndof} L^2 \sqrt{\rho_0 A_0 / I_0 E_0}$ and ordinate axis corresponds to the normalized maximum amplitude $A^*_{\max} = A_{\max} / R$.

Figures 8-10 illustrate the backbone curves, respectively for beams 1, 2 and 3 with α = 0.4 and for different values of n_M, different positions x_n and magnitudes η_n of the point masses. It can observe that the effect of non-linearity increases or decreases by varying the position, number and magnitude of the added masses.

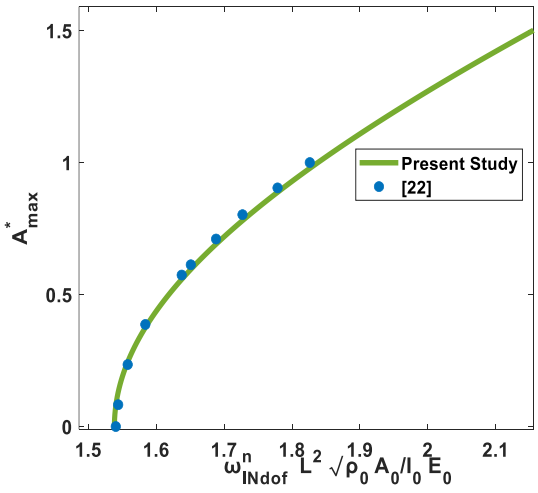

Figure 6. Backbone curves corresponding to uniform beam containing 3 spots masses

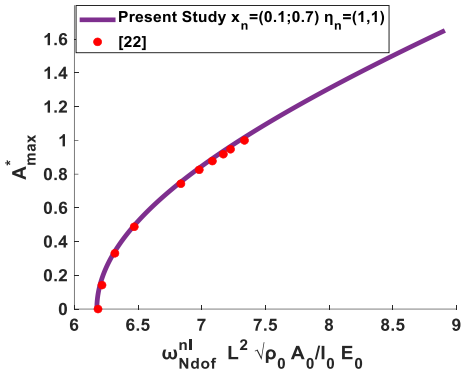

Figure 7. Backbone curves corresponding to uniform beam containing 2 spots masses

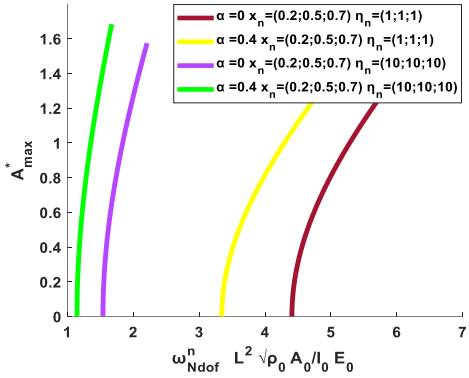

Figure 8. Comparison of the backbone curves corresponding to (beam 1) containing 3 spots masses for different values of α

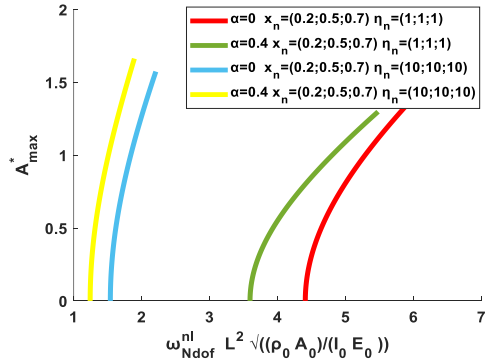

Figure 9. Comparison of the backbone curves corresponding to (beam 2) containing 3 spots masses for different values of α

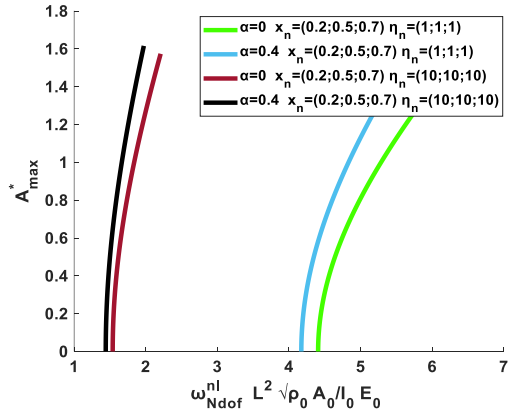

Figure 10. Comparison of the backbone curves corresponding (beam 3) containing 3 spots masses for different values of α

3.2. Numerical Result 2

In this paragraph we provide the results of the dimensionless nonlinear frequencies for the (TAFGB) containing masses at various spots. The large amplitude free vibration behavior is illustrated by backbone curves in the dimensionless maximum amplitude-frequency plane. The beam is supposed to be exponentially tapered with constant width and variable thickness according to the law $h(x) = h_0 \exp(-\beta\sqrt{x/L})$ for $0 \le x \le L$. This allows us to rewrite the expression of the cross-section and the squared moment as $A(x) = A_0 \exp(-\beta\sqrt{x/L})$ and $I(x) = I_0 \exp(-\beta\sqrt{x/L})^3$. The laws of change of the material characteristics are presented in Table 2.

Table 2. The laws of variation of physical properties of AFG tapered beams

Material 1	$E(x) = E_0$	$\rho(x) = \rho_0$
Material 2	$E(x) = E_0(\frac{x}{L}+1)$	$\rho(x) = \rho_0((\frac{x}{L})^2 + \frac{x}{L}+1)$

Figures 11 and 12 show the backbone curves in terms of the maximum dimensionless amplitude $A^*_{\max} = A_{\max}/R$ as a function of the ratio of nonlinear and linear dimensionless frequencies $\omega^{*nl}_{Ndof}/\omega^{*l}_{Ndof}$ of the exponentially tapered axial gradient beam according respectively to material 1 and 2 for different values of β.

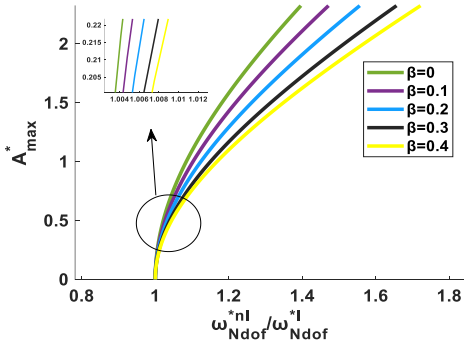

Figure 11. Backbone curves corresponding to beam presented in section 3.2 according to material 1 for different value of β

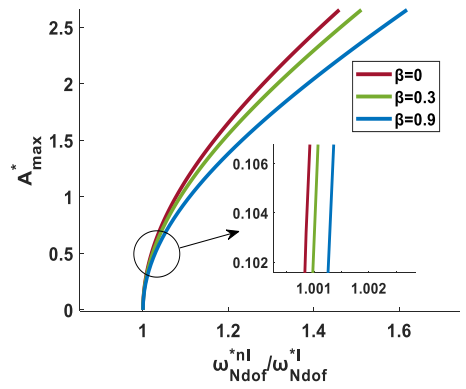

Figure 12. Backbone curves corresponding to beam presented in section 3.2 according to material 2 for different value of β

The non-linearity is more important for the (TAFGB) made of material 2 than for beams made of material 1. Because the stiffness of the longitudinal springs modeling the geometric nonlinearity of material 2 is greater than that of material 1. To illustrate the effect of the additions of masses on the backbone curve of the (TAFGB) we take the example of an AFG beam according to material 2 and whose thickness follows the parabolic law $h(x)=h_0(1-\mu(x/L)^2)$ carrying 3-point masses i.e. $n_M=3$, respectively at $x_n=(0.2L;0.5L;0.7L)$ and $\eta_n=(10;10;10)$ and μ is the taper ratio of the considered beam as Figure 13.

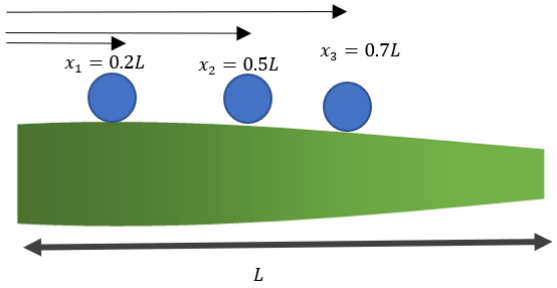

Figure 13. The parabolically tapered beam containing 3 spots masses

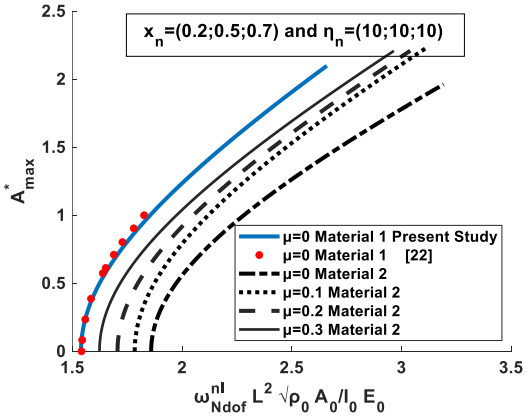

Figure 14. Comparison of the backbone curves corresponding the parabolically tapered beam presented in section 3.2 containing 3 spots masses

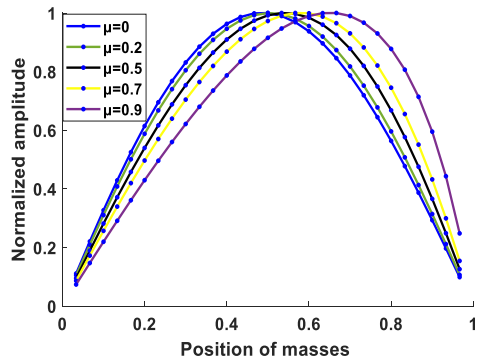

Figure 15. The first linear mode shape related to (beam 3) containing 3-point masses

Figure 14 shows the backbone curve of the considered beam. This model allows a good understanding of the dynamic behavior of the (TAFGB) by putting the mass in any place in it, this can be changing the mass matrix presented in Equation (24). In Figure 15, we present the first linear mode shape corresponding to beam presented in section 3.1 according to material 2 for different values of μ, carrying 3-point masses at various places.

Figure 13 presents the first linear mode shape related of beam presented in section 3.2 for different values of the taper ration β. It can be seeing the effect of the parameter beta on the first mode curve.

5. CONCLUSION

The discrete model, is used to give nonlinear frequencies of the (TAFGB) containing arbitrary number point masses in various locations. The numerical formulation of this method has been presented and the formula for the new tensors m_{ij}, k_{ij} and b_{ijkl} have been developed. The application was concerned with simply (TAFGB) extremity. The results of the dimensionless frequencies $\omega^{*nl}_{Ndof}/\omega^{*l}_{Ndof}$ were obtained by applying a single mode approach. the results for the dimensionless frequency of the (TAFGB) in good agreement with other previously published which ensuring the edibility of the new mechanical model. This model allows the prediction of large amplitude vibration frequencies for any types of conical beam and for any combination of functional gradient materials. The best choice of a number (N-Dof) that gives a minimum of error almost for all applications is N=29.

REFERENCES

[1] E. Guliyev, "Vibrations of a Moving Fluid-Contacting Three-Dimensional Cylinder Stiffened with Rods", International Journal on Technical and Physical Problems of Engineering (IJTPE), Issue 42, Vol. 12, No. 1, pp. 68-72, March 2020.

[2] R.N. Agayev, 'Vibrations of an Inhomogeneous Cylindrical Shell Dynamically Interacting with Motive Fluid and Stiffened with Rings", International Journal on Technical and Physical Problems of Engineering (IJTPE), Issue 42, Vol. 12, No. 1, pp. 31-34, March 2020.

[3] Z.M. Badirov, "Vibrations of an Orthotropic, Heterogeneous Cylindrical Shell Dynamically Contacting with Viscous Liquid and Stiffened with Bars", International Journal on Technical and Physical Problems of Engineering (IJTPE), Issue 46, Vol. 13, No. 1, pp. 18-22, March 2021.

[4] F.T. Mamedrzayeva, "Free Vibrations of an Orthotropic Cylindrical Shell Stiffened with Cross Systems of Ribs, with Medium and Fluid Cross Systems", International Journal on Technical and Physical Problems of Engineering (IJTPE), Issue 42, Vol. 12, No. 1, pp. 58-62, March 2020.

[5] A.H. Movsumova, "Free Vibration of Inhomogeneous, Orthotropic and Medium-Contacting Culindrical Panel

Stiffened with Annular Ribs", International Journal on Technical and Physical Problems of Engineering (IJTPE), Issue 42, Vol. 12, No. 1, pp. 40-43, 2020.
[6] O. Outassafte, A. Adri, Y. El Khouddar, S. Rifai, R. Benamar, "Geometrically Non-Linear Free and Forced Vibration of a Shallow Arch", J. Vibroeng., Vol. 23, No. 7, pp. 1508-1523, November 2021.
[7] O. Outassafte, A. Adri, Y.E. Khouddar, S. Rifai, R. Benamar, "Geometrically Non-Linear Free In-Plane Vibration of Circular Arch Elastically Restrained Against Rotation at the two Ends", IJETT, Vol. 69, No. 3, pp. 85-95, March 2021.
[8] F.T. Mammadrzayeva, 'Natural Vibrations of an Orthotropic Cylindrical Shell-Solid-Fluid Stiffened with Annular Ribs", International Journal on Technical and Physical Problems of Engineering (IJTPE), Issue 45, Vol. 12, No. 4, pp. 6-10, December 2020.
[9] A. Moukhliss, A. Rahmouni, O. Bouksour, R. Benamar, "N-Dof Discrete Model to Investigate Free Vibrations of Cracked Tapered Beams and Resting on Winkler Elastic Foundations", International Journal on Technical and Physical Problems of Engineering (IJTPE), Issue 50, Vol. 14, No. 1, pp. 71-77, March 2022.
[10] N. Shafiei, M. Kazemi, M. Ghadiri, "Nonlinear Vibration of Axially Functionally Graded Tapered Microbeams", International Journal of Engineering Science, Vol. 102, pp. 12-26, May 2016.
[11] S. Sinir, M. Cevik, B.G. Sinir, "Nonlinear Free and Forced Vibration Analyses of Axially Functionally Graded Euler-Bernoulli Beams with Non-Uniform Cross-Section", Composites Part B: Engineering, Vol. 148, pp. 123-131, September 2018.
[12] K. Xie, Y. Wang, T. Fu, "Dynamic Response of Axially Functionally Graded Beam with Longitudinal–Transverse Coupling Effect", Aerospace Science and Technology, Vol. 85, pp. 85-95, February 2019.
[13] A. Moukhliss, A. Rahmouni, O. Bouksour, R. Benamar, 'Using the Discrete Model for the Processing of Natural Vibrations, Tapered Beams Made of AFG Materials Carrying Masses at Different Spots", Materials Today: Proceedings, Vol. 52, pp. 21-28, 2022.
[14] A. Rahmouni, Z. Beidouri, R. Benamar, "A Discrete Model for Geometrically Nonlinear Transverse Free Constrained Vibrations of Beams with Various end Conditions", Journal of Sound and Vibration, Vol. 332, No. 20, pp. 5115-5134, September 2013.
[15] A. Khnaijar, R. Benamar, "A Discrete Model for Nonlinear Vibrations of a Simply Supported Cracked Beams Resting on Elastic Foundations", Vol. 18, No. 3, p. 8, 2017.
[16] A. Rahmouni, Z. Beidouri, R. Benamar, "A Discrete Model for the Natural Frequencies and Mode Shapes of Constrained Vibrations of Beams with Various Boundary Conditions", Matec Web of Conferences, Vol. 1, p. 10015, 2012.
[17] M. El Kadiri, R. Benamar, R.G. White, "Improvement of the Semi-Analytical Method, for Determining the Geometrically Non-Linear Response of Thin Straight Structures. Part I: Application to Clamped-Clamped and Simply Supported-Clamped Beams", Journal of Sound and Vibration, Vol. 249, No. 2, pp. 263-305, 2002.
[18] A. Rahmouni, Z. Beidouri, R. Benamar, "A Discrete Model for Geometrically Nonlinear Transverse Free Constrained Vibrations of Beams with Various end Conditions", Journal of Sound and Vibration, Vol. 332, No. 20, pp. 5115-5134, September 2013.
[19] K.K. Raju, B.P. Shastry, G.V. Rao, "A Finite Element Formulation for the Large Amplitude Vibrations of Tapered Beams", Journal of Sound and Vibration, Vol. 47, No. 4, pp. 595-598, August 1976.
[20] A. Rahmouni, R. Benamar, "A Discrete Model for Geometrically Non-Linear Transverse Free Constrained Vibrations of Beams Carrying a Concentrated Mass at Various Locations", p. 8, 2014.
[21] L.S. Raju, G.V. Rao, K.K. Raju, "Large Amplitude free Vibrations of Tapered Beams", AIAA Journal, Vol. 14, No. 2, pp. 280-282, 1976.
[22] E. Ozkaya, "Non-Linear Transverse Vibrations of a Simply Supported Beam Carrying Concentrated Masses", Journal of Sound and Vibration, Vol. 257, No. 3, pp. 413-424, October 2002.

BIOGRAPHIES

Anass Moukhliss was born in Casablanca, Morocco in 1995. He received the Master degree in mechanical energy from University Hassan II of Casablanca, Morocco in 2018. Currently, he is a Ph.D. student at National Higher School, Electricity and Mechanics, (ENSEM), Hassan II University, Casablanca, Morocco. He is the member of Mechanics, Production and Industrial Engineering (LMPGI) laboratory. His research interest is in mechanical engineering, and numerical modeling of structures.

Abdellatif Rahmouni was born in Berrechid, Morocco in 1963. He got the engineering degree in Design and Mechanical Manufacturing in 1989 and Ph.D. degree in Applied Science, Specialty of Simulation, Instrumentation and Measurement from Mohammadia School of Engineers (EMI), Mohammed V University, Rabat, Morocco. He is a Professor of Mechanical Engineering at Superior School of Technology (EST), University of Hassan II, Casablanca, Morocco. His research interest is in mechanical engineering, numerical modeling of structures.

Otmane Bouksour was born in Rabat, Morocco in 1957. He received the Eng. degree in Civil Engineering from Mohammadia School of Engineers, University of Mohamed V, Rabat Morocco in 1981 and the M.Sc. and Ph.D. degrees in Structures and Mechanic of Solids from University of Sherbrooke, Quebec, Canada in 1986 and 1990, respectively. Currently, he is a Professor at Mechanical Engineering Department, High Scholl of Technology, University of Hassan II, Casablanca Morocco. His research interest is in industrial engineering, logistics and numerical modeling of structures.

Rhali Benamar was born in Fes, Morocco in 1960. He got the engineering degree in civil engineering from National School of Bridges and Roads, Paris, France in 1982. He received the Ph.D. degree from Institute of Sound and Vibration at the University of Southampton, UK in 1990. Currently, he is a Professor of Mechanical Engineering and Vibrations at Mohammadia School of Engineering (EMI), Mohammed V University, Rabat, Morocco. His research interest is in mechanical engineering, numerical modeling of structures.